JOURNAL OF MATERIALS SCIENCE **38** (2003) 1853–1857

Electrical characteristics of $Sr_xBi_{2.4}Ta_2O_9$ thin film and Pt/$Sr_{0.85}Bi_{2.4}Ta_2O_9$/Al_2O_3/Si structure

JI-WOONG KIM, JAE-HOON CHOI, TAE-SUNG OH
Department of Materials Science and Engineering, Hong-Ik University, Seoul 121-791, Korea
E-mail: oht@hongik.ac.kr

$Sr_xBi_{2.4}Ta_2O_9$ ($0.7 \leq x \leq 1.3$) thin films were processed by metalorganic decomposition and their ferroelectric characteristics were investigated. The Sr-deficient $Sr_xBi_{2.4}Ta_2O_9$ films exhibited well-developed ferroelectric hysteresis curves compared to those of the Sr-excess films, and $Sr_{0.85}Bi_{2.4}Ta_2O_9$ film had the optimum electrical characteristics among $Sr_xBi_{2.4}Ta_2O_9$ films. Electrical characteristics of the Pt/SBT/Al_2O_3/Si structure using $Sr_{0.85}Bi_{2.4}Ta_2O_9$(SBT) film were investigated for metalferroelectric-insulator-semiconductor field-effect-transistor (MFIS-FET) applications. Memory window of C-V hysteresis characteristics of the Pt/SBT/Al_2O_3/Si structure became large with decreasing the Al_2O_3 thickness, and the Pt/SBT(400 nm)/Al_2O_3 (10 nm)/Si structure gave memory window of 2.2 V at sweeping voltages of $\pm$5 V. The Pt/SBT/Al_2O_3/Si structure can be proposed for MFIS-FET applications.

1. Introduction

Recently, ferroelectric thin films of bismuth layered perovskite structure such as $SrBi_2Ta_2O_9$ have been extensively investigated for non-volatile ferroelectric random access memory (FRAM) applications due to their fatigue-free characteristics and possibility of low switching voltage [1–4]. Ferroelectric characteristics of $SrBi_2Ta_2O_9$ films are largely dependent on the composition of the films [5–7], and it has been reported that the remanent polarization of $SrBi_2Ta_2O_9$ thin films can be controlled by Sr/Bi mole ratio of the films [8, 9]. In this work, $Sr_xBi_{2.4}Ta_2O_9$ thin films were processed by metalorganic decomposition (MOD) with varying the Sr content x within the range of 0.7–1.3, and ferroelectric characteristics of the $Sr_xBi_{2.4}Ta_2O_9$ films were investigated.

Ferroelectric field-effect-transistor is one of the most promising candidates for future nonvolatile memories, because non-destructive readout is possible with high density integration and large remanent polarization of ferroelectric film is not required [10, 11]. Although metal-ferroelectric-semiconductor field-effect-transistor (MFS-FET) has been studied for over 30 years, reliable products have not been demonstrated, as elements in the ferroelectric films diffuse into Si and degrade the interface characteristics [12, 13]. As an alternative solution, metal-ferroelectric-insulator-semiconductor (MFIS) structure has been proposed [14–16] to improve the interfacial properties using buffer layer such as CeO_2, Y_2O_3, $SrTiO_3$, and TiO_2.

In this work, we have prepared the Pt/SBT/Al_2O_3/Si structure using $Sr_{0.85}Bi_{2.4}Ta_2O_9$ (SBT) film, which exhibited the optimum electrical properties among $Sr_xBi_{2.4}Ta_2O_9$ films, and investigated the electrical properties of the Pt/SBT/Al_2O_3/Si structure with variation of the Al_2O_3 thickness. Although $SrBi_2Ta_2O_9$ thin film has attracted much attention for FRAM applications due to its fatigue-free characteristics and a small coercive field, high annealing temperature such as 800°C is needed to obtain the optimum ferroelectric properties [1]. Thus, buffer material for MFIS structure with SBT film should be stable and thickness of the buffer layer should be thick enough to prevent interdiffusion between SBT film and Si during such high-temperature annealing process. Al_2O_3 is very stable oxide [6] and offers relatively high dielectric constant [17, 18]. Thus, it is expected that Al_2O_3 acts as a good diffusion barrier and exhibits a low gate voltage even with sufficient thickness.

2. Experimental procedure

As bismuth volatility occurs during annealing process of the MOD-derived SBT film, addition of excess bismuth oxide into the coating solutions is required to prevent the bismuth deficiency of the film. Sr-2-ethylhexanoate, Bi-2-ethylhexanoate, and Ta-2-ethylhexanoate of 0.5 M concentration were mixed as Sr:Bi:Ta mole ratio of x:2.4:2 ($0.7 \leq x \leq 1.3$), and diluted with n-butyl acetate to make the MOD coating solutions of 0.05 M concentration. $Sr_xBi_{2.4}Ta_2O_9$ films were deposited on the Pt/Ti/SiO_2/Si substrates by spin-coating at 3000 rpm for 30 sec, and spin-coated films were dried at 400°C for 10 min in air. This procedure was repeated to obtain the desired film thicknesses of 200 nm and 400 nm. Finally, the films were annealed at 800°C for 1 hr in oxygen ambient. Pt top electrodes of 200 μm diameter and 200 nm thickness were sputtered on the annealed film surface at room temperature, and post annealing of the films was conducted using RTA

at 600°C for 10 min in oxygen ambient to stabilize the Pt/SBT interface.

To fabricate the Pt/SBT/Al_2O_3/Si structures, Al_2O_3 buffer layers of 10–50 nm thickness were deposited on RCA-cleaned p-type Si substrates using DC reactive sputtering at room temperature. During sputter-deposition of Al_2O_3 films, the oxygen content in the sputtering gas ($Ar + O_2$) was kept as 50%. Then, $Sr_{0.85}Bi_{2.4}Ta_2O_9$ film and Pt top electrodes were fabricated on the Al_2O_3/Si with the same procedure described above. Native oxide on the backside of the Si substrate was etched using buffered hydrofluoric acid, and aluminum was sputtered for ohmic contact. Consequently, Pt(200 nm)/SBT(400 nm)/Al_2O_3(10–50 nm)/Si structures were prepared.

Crystalline phases of $Sr_xBi_{2.4}Ta_2O_9$ films and the SBT/Al_2O_3/Si structure were characterized by X-ray diffractometry (XRD). Remanent polarization and coercive field of $Sr_xBi_{2.4}Ta_2O_9$ films were characterized using RT66A ferroelectric tester. C-V characteristics of the Pt/SBT/Al_2O_3/Si structure were measured by HP 4194A. Leakage current density of $Sr_xBi_{2.4}Ta_2O_9$ films and the Pt/SBT/Al_2O_3/Si structure was measured by HP 4194A.

3. Results and discussion

3.1. Characteristics of $Sr_xBi_{2.4}Ta_2O_9$ film

Fig. 1 shows the XRD patterns of the 200 nm-thick $Sr_xBi_{2.4}Ta_2O_9$ films. As reported that the Sr-deficient $SrBi_2Ta_2O_9$ ceramics maintain bismuth layered perovskite structure by Bi substitution to Sr sites [8, 19], the MOD-derived $Sr_xBi_{2.4}Ta_2O_9$ thin films with the Sr content ranging from 0.7 to 1.0 were fully crystallized to bismuth layered perovskite structure by annealing at 800°C for 1 h in oxygen ambient. For the films with the Sr content larger than 1.0, however, decrease in (115) peak intensity and increase in peak broadening were observed with increasing the Sr content.

As illustrated in Fig. 2, ferroelectric hysteresis curves of the 200 nm-thick $Sr_xBi_{2.4}Ta_2O_9$ films became severely deteriorated with increasing the Sr content x to 1.15 and 1.3. The skinny hysteresis curves

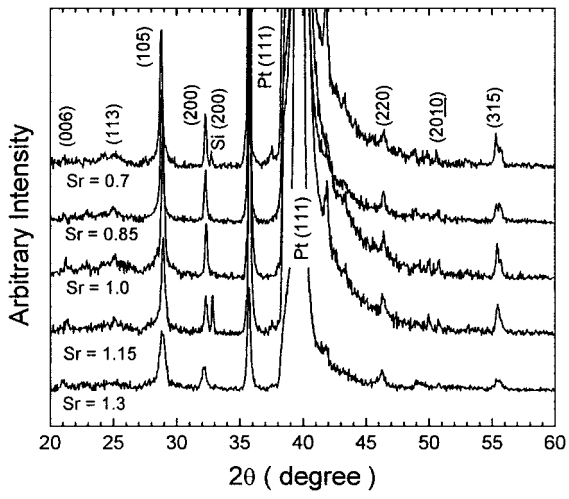

Figure 1 XRD patterns of $Sr_xBi_{2.4}Ta_2O_9$ films after annealing at 800°C for 1 hr in oxygen ambient.

with extremely low remanent polarization for the $Sr_xBi_{2.4}Ta_2O_9$ films with the Sr content x of 1.15 and 1.3 were considered to be due to their poor crystallization, as shown in Fig. 1.

Fig. 3 shows the remanent polarization ($2P_r$) of $Sr_xBi_{2.4}Ta_2O_9$ films as a function of the Sr content x. $2P_r$ of 400 nm-thick films were also plotted in Fig. 3. As clearly seen for 200 nm-thick films, $2P_r$ of the MOD-derived $Sr_xBi_{2.4}Ta_2O_9$ films was maximized at the Sr content x of 0.85. Such result was well consistent with other's works [9, 20] and could be supported by the report that Bi substitution and the cation vacancies at the Sr sites enhance the structural distortion in the TaO_6 octahedra and lead to the larger polarization in the Sr-deficient $SrBi_2Ta_2O_9$ films [8]. In Fig. 3, remanent polarization ($2P_r$) of the $Sr_xBi_{2.4}Ta_2O_9$ films increased with decreasing the film thickness at the same sweeping voltage of ±5 V, which was due to the fact that ferroelectric characteristics of thin films are dependent upon the electric field rather than the applied voltage. The 200 nm-thick $Sr_{0.85}Bi_{2.4}Ta_2O_9$ film exhibited $2P_r$ of 24.0 μC/cm^2 and E_c (coercive field) of 57 kV/cm at sweeping voltage of ±5 V, and the 400 nm-thick $Sr_{0.85}Bi_{2.4}Ta_2O_9$ film exhibited $2P_r$ of 10.2 μC/cm^2 and E_c of 37.5 kV/cm at sweeping voltage of ±5 V.

Leakage current density of the 200 nm-thick $Sr_xBi_{2.4}Ta_2O_9$ films is plotted in Fig. 4 as a function of the applied electric field. Increase in the leakage current density and decrease in breakdown field were observed with increasing the Sr content x. With these results, it was found out that $Sr_{0.85}Bi_{2.4}Ta_2O_9$ film possessed the optimum electrical properties among $Sr_xBi_{2.4}Ta_2O_9$ films.

3.2. Characteristics of the Pt/SBT/Al_2O_3/Si structure

The Pt/SBT/Al_2O_3/Si structure was prepared using $Sr_{0.85}Bi_{2.4}Ta_2O_9$ film, as this has the optimum electrical properties among $Sr_xBi_{2.4}Ta_2O_9$ films. Referring to the previous work [21] on the Pt/$SrBi_{2.4}Ta_2$/TiO_2/Si structure, the memory window has been reported to become larger with increasing the $SrBi_{2.4}Ta_2O_9$ film thickness. Thus, 400 nm-thick $Sr_{0.85}Bi_{2.4}Ta_2O_9$ film rather than 200 nm-thick film was used for the Pt/SBT/Al_2O_3/Si structure.

Fig. 5 shows the XRD patterns of the 400 nm-thick $Sr_{0.85}Bi_{2.4}Ta_2O_9$(SBT) films prepared on the as-deposited Al_2O_3(50 nm)/Si and Pt/Ti/SiO_2/Si substrates followed by annealing at 800°C for 1 h in oxygen atmosphere. The MOD-derived SBT films on the Al_2O_3/Si and platinized Si substrates were fully crystallized to bismuth layered perovskite structure without preferred orientation. XRD patterns of the SBT film prepared on the Al_2O_3/Si substrate were identical to those prepared on the Pt/Ti/SiO_2/Si substrate, indicating that the crystallization behavior of the MOD-derived SBT film was not much affected with the underlayer.

C-V curves of the Pt/SBT(400 nm)/Al_2O_3(10 nm)/Si structure were shown in Fig. 6. Within the sweeping voltage range of ±3 V–±7 V, the Pt/SBT/Al_2O_3/Si

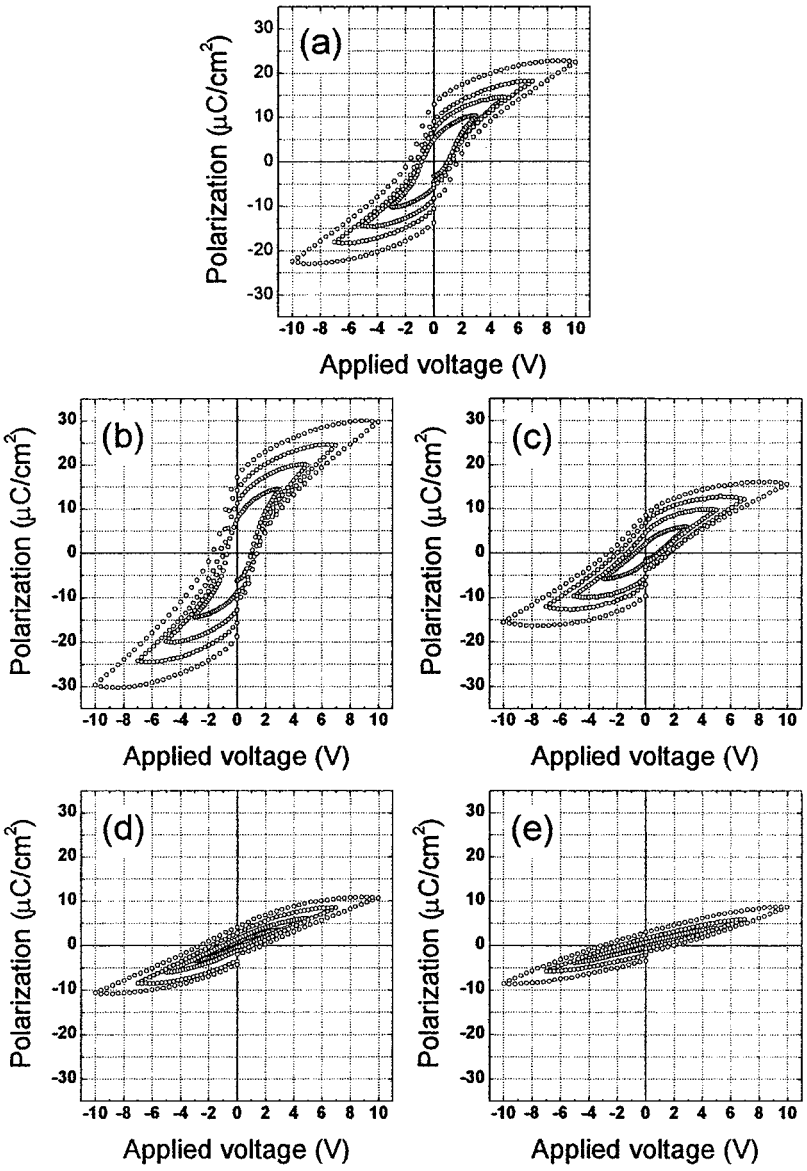

Figure 2 Ferroelectric hysteresis curves of $Sr_xBi_{2.4}Ta_2O_9$ films with the Sr content x of (a) 0.7, (b) 0.85, (c) 1.0, (d) 1.15, and (e) 1.3.

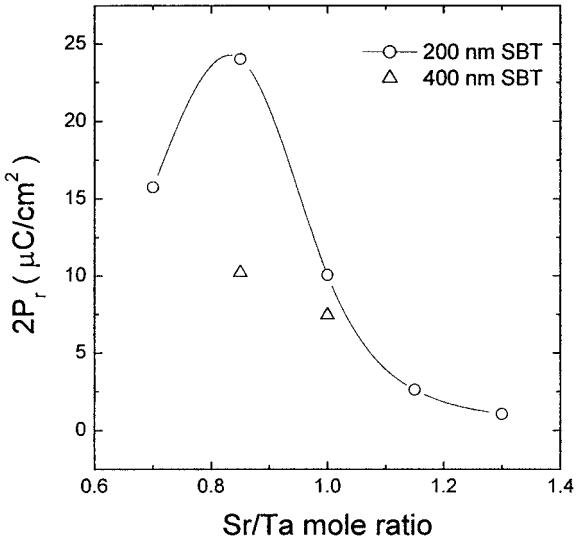

Figure 3 Remanent polarization ($2P_r$) of $Sr_xBi_{2.4}Ta_2O_9$ films with the Sr content x of (a) 0.7, (b) 0.85, (c) 1.0, (d) 1.15, and (e) 1.3 at the sweeping voltage of ±5 V.

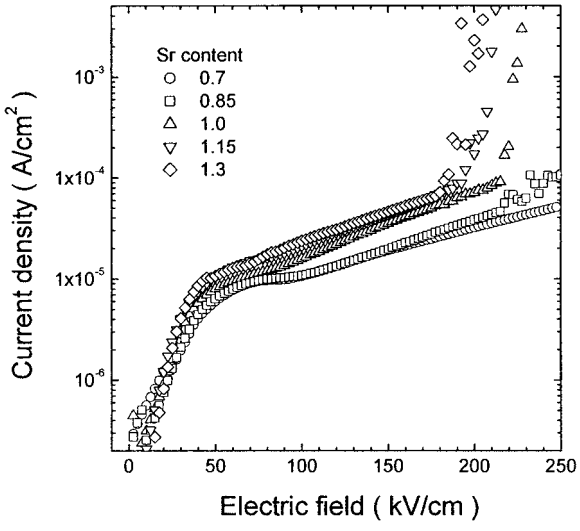

Figure 4 Leakage current density of $Sr_xBi_{2.4}Ta_2O_9$ films as a function of the applied electric field.

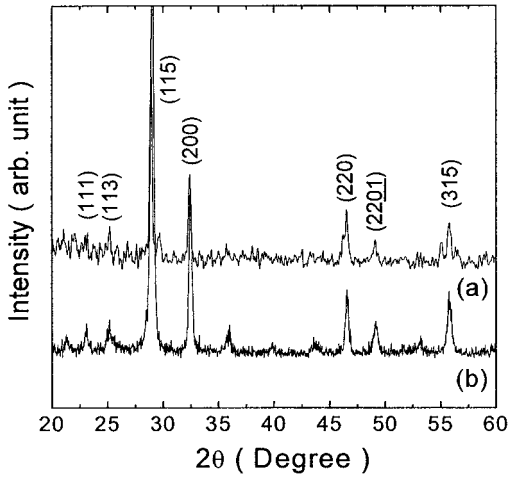

Figure 5 XRD patterns of $Sr_{0.85}Bi_{2.4}Ta_2O_9$ films prepared on the (a) Al_2O_3/Si and (b) Pt/Ti/SiO_2/Si substrates.

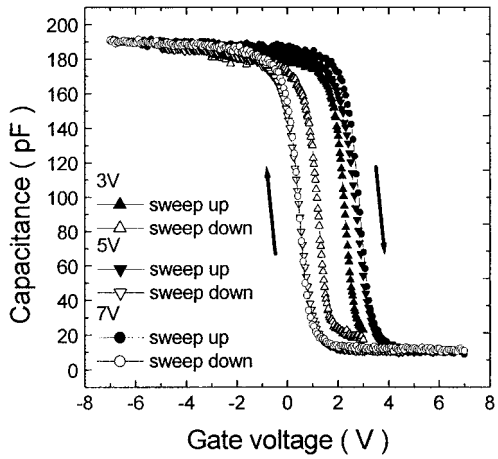

Figure 6 C-V curves of the Pt/SBT(400 nm)/Al_2O_3(10 nm)/Si structure.

structure with 10 nm-thick Al_2O_3 buffer layer exhibited clockwise directional hysteresis, indicating the well-defined ferroelectric switching behavior of the SBT film. In the C-V curves in Fig. 6, the memory window, which is the width of threshold voltage, became larger with increase of the sweeping voltage from ±3 V to ±7 V. Increase in the memory window with increasing the sweeping voltage was due to the fact that the electric field on the SBT film is determined by the gate voltage.

The memory window of the MFIS structure is related to the coercive field of the ferroelectric film, as expressed in Equation 1,

$$\Delta V_{\text{window}} = 2d_{\text{f}} \cdot E_{\text{c}} \tag{1}$$

where ΔV_{window} is the memory window of the MFIS, d_{f} is thickness of the ferroelectric film [11]. Memory window of the Pt/SBT(400 nm)/Al_2O_3(10 nm)/Si structure was lower than the value estimated using Equation 1, which might be caused by small charge injection into the SiO_2 layer formed during annealing process of the SBT film. It is well known that SiO_2 layer is easily formed at the interface between buffer oxide and Si during annealing at high temperatures such as 800°C [22].

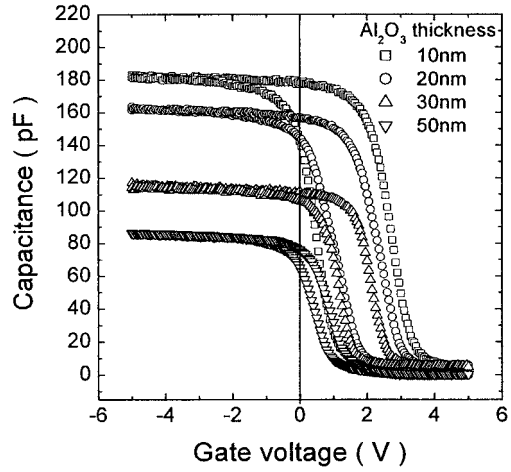

Figure 7 C-V curves of the Pt/SBT/Al_2O_3/Si structures with 10–50 nm Al_2O_3 layer.

Fig. 7 shows the C-V curves of Pt/SBT/Al_2O_3/Si structures with 10–50 nm Al_2O_3 buffer layers. The bias voltage was applied at a sweep rate of 0.05 V/sec from −5 V to +5 V and vice versa. The C-V curves of the Pt/SBT/Al_2O_3/Si structures show hysteresis loops with clockwise rotation regardless of the Al_2O_3 thickness ranging from 10 nm to 50 nm. The maximum capacitance and the memory window of the Pt/SBT/Al_2O_3/Si structure decreased with increasing the thickness of the Al_2O_3 buffer layer. Thickness increase of the Al_2O_3 buffer layer with lower dielectric constant causes a reduction of the electric field on the SBT film, resulting in a reduction of the memory window of the Pt/SBT/Al_2O_3/Si structure [19]. The maximum memory window of the Pt/SBT/Al_2O_3(10 nm)/Si structure was observed to be about 2.2 V at the sweeping voltage of ±5V.

In Fig. 7, a shift of the flatband voltage to positive voltage was observed due to the negative charges fixed in the oxide layer [7]. Such negative charges were produced by formation of SiO_2 at the Al_2O_3/Si interface during annealing process at 800°C. Although annealing was conducted in oxygen ambient, formation of SiO_2 at the Al_2O_3/Si interface could extract oxygen from the Al_2O_3 layer and generate oxygen vacancies in the Al_2O_3 layer. With formation SiO_2 at the Al_2O_3/Si interface, the Pt/SBT/Al_2O_3/Si structure could be considered as a series capacitor with the components of SBT, Al_2O_3, and SiO_2. Capacitance in the accumulation region, C_{max}, of the Pt/SBT/Al_2O_3/Si structure was estimated using Equation 2 and compared with the measured value.

$$1/C_{\text{max}} = 1/C_{\text{f}} + 1/C_{\text{i}} + 1/C_{\text{SiO}_2} \tag{2}$$

where C_{max} is the capacitance in the accumulation region, C_{f} is the capacitance of SBT film, C_{i} is the capacitance of Al_2O_3 layer, and C_{SiO_2} is the capacitance of SiO_2 layer. Fig. 8 shows that C_{max} of the Pt/SBT/Al_2O_3/Si structure increased with decreasing the Al_2O_3 thickness and 3 nm-thick SiO_2 layer was formed at the Al_2O_3/Si interface.

Leakage current characteristics of the Pt/SBT/Al_2O_3/Si structure are plotted as a function of the Al_2O_3

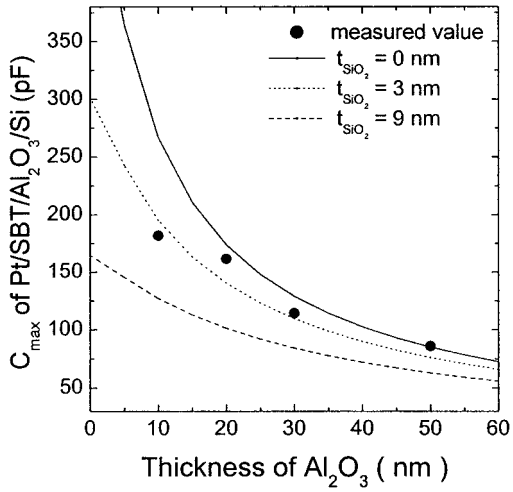

Figure 8 C_{max} of the Pt/SBT/Al_2O_3/Si structures with various Al_2O_3 thickness.

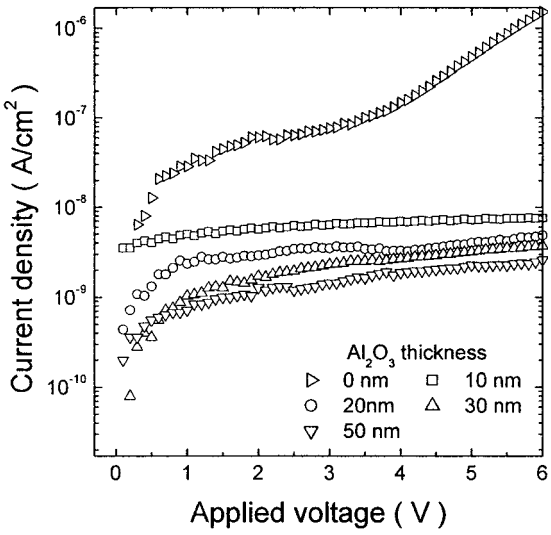

Figure 9 Leakage current density of the Pt/SBT/Al_2O_3/Si structure.

layer thickness in Fig. 9. Also, the leakage current density of the Pt/SBT/Si structure without the Al_2O_3 buffer layer is compared in Fig. 9. Leakage current density of the Pt/SBT/Al_2O_3/Si structure decreased with increasing the Al_2O_3 layer thickness and was about 7.56×10^{-9} A/cm^2 at 6 V for the Pt/SBT(400 nm)/Al_2O_3(10 nm)/Si structure. On the contrary, the Pt/SBT/Si structure without the Al_2O_3 buffer layer showed much higher leakage current density, implying that the interfacial characteristics were substantially improved by inserting the Al_2O_3 film as a buffer layer between SBT and Si.

4. Conclusions

(1) The Sr-deficient $Sr_xBi_{2.4}Ta_2O_9$ films exhibited well-developed ferroelectric hysteresis curves compared to those of the Sr-excess $Sr_xBi_{2.4}Ta_2O_9$ films.

(2) $Sr_{0.85}Bi_{2.4}Ta_2O_9$ film has the optimum electrical characteristics among $Sr_xBi_{2.4}Ta_2O_9$ films. The 200 nm-thick $Sr_{0.85}Bi_{2.4}Ta_2O_9$ film exhibited $2P_r$ of 24.0 μC/cm^2 and E_c of 57 kV/cm at $\pm$5 V, and the 400 nm-thick $Sr_{0.85}Bi_{2.4}Ta_2O_9$ film exhibited $2P_r$ of 10.2 μC/cm^2 and E_c of 37.5 kV/cm at $\pm$5 V.

(3) We verified that Al_2O_3 thin film was suitable as a buffer layer for deposition of SBT film on Si substrate to prepare the MFIS structure. The Pt/SBT/Al_2O_3/Si structure can be proposed for MFIS-FET applications.

(4) Memory window of the Pt/SBT/Al_2O_3/Si structure became larger with decreasing the Al_2O_3 thickness, and the Pt/SBT(400 nm)/Al_2O_3 (10 nm)/Si structure exhibited C-V hysteresis characteristics with a memory window of 2.2 V at $\pm$5 V.

Acknowledgement

This work was supported by Center for Electronic Packaging Materials of Korea Science and Engineering Foundation.

References

1. J. F. SCOTT and C. A. ARAUJO, *Science* **246** (1990) 1400.
2. K. WATANABE, A. J. HARTMAN, R. N. LAMB and J. F. SCOTT, *J. Appl. Phys.* **84** (1998) 2170.
3. D. J. YEON, J. D. PARK and T. S. OH, *J. Kor. Phys. Soc.* **30** (1998) S173.
4. Y. ZHU, S. B. DESU, T. LI and S. RAMANATHAN, *J. Mater. Res.* **12** (1998) 783.
5. I. KOIWA, Y. OKADA, J. MITA, A. HASHIMOTO and Y. SAWADA, *Jpn. J. Appl. Phys.* **36** (1997) 5904.
6. H. TSAI, P. LIN and T. TSENG, *J. Appl. Phys.* **85** (1999) 1095.
7. S. BHATTACHAYA, A. R. JAMES and S. B. KRYPHANIDHI, *Solid State Comm.* **108** (1998) 759.
8. Y. SHIMAKAWA, Y. KUBO, N. NAKAGAWA, T. KAMIYAMA, H. ASANO and F. IZUMI, *Appl. Phys. Lett.* **74** (1999) 1904.
9. K. WATANABE, M. TANAKA, E. SUMITOMO, K. KATORI, H. YAGI and J. F. SCOTT, *ibid.* **73** (1998) 126.
10. E. TOKUMITSU, D. TAKAHASHI and H. ISHIWARA, *Jpn. J. Appl. Phys.* **39** (2000) 5456.
11. T. KANASHIMA and M. OKUYAMA, *ibid.* **38** (1999) 2044.
12. Y. MATSUI, M. OKUYAMA, M. NODA and Y. HAMAKAWA, *Appl. Phys.* A **28** (1982) 161.
13. W. J. LEE, B. G. YU, J. S. LYU, J. H. LEE and B. W. KIM, *J. Kor. Phys. Soc.* **35** (1999) 509.
14. H. N. LEE, Y. T. KIM and S. H. CHOH, *ibid.* **34** (1999) 454.
15. E. TOKUMITSU, K. ITANI, B. MOON and H. ISHIWARA, *Jpn. J. Appl. Phys.* **34** (1995) 5202.
16. J. D. PARK and T. S. OH, *J. Kor. Phys. Soc.* **37** (2000) 1072.
17. K. P. PANDE, V. K. R. NAIR and D. GUTIERREZ, *J. Appl. Phys.* **54** (1983) 5436.
18. K. D. SCHRODER, in "Semiconductor Materials and Device Characterization" 2nd ed., Chap. 6 (John Wiley & Sons, New York, 1998) p. 27.
19. K. MIURA and M. TANAKA, *Jpn. J. Appl. Phys.* **37** (1998) 2554.
20. T. ATSUKI, N. SOYAMA, T. YONEZAWA and K. OGI, *ibid.* **34** (1995) 5096.
21. J. W. KIM, K. W. LEE, J. H. CHOI and T. S. OH, "Abstract Book of MRS Spring Meeting" (Mater. Res. Soc., San Francisco, 2001) p. 124.
22. J. SENZAKI, K. KURIHARA, N. NOMURA and O. MITSUNAGA, *Jpn. J. Appl. Phys.* **37** (1998) 5150.

Received 10 December 2002
and accepted 26 February 2003